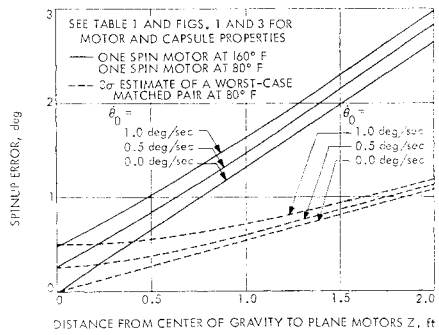

Fig. 7 Results of calculations for pointing error caused by spin-up.

3σ estimates of worst-case spin-motor mismatch (Table 1) were then employed to generate simulated pressure-time curves which served as the forcing function for the motion of the capsule. Since the spin motors weighed approximately 1 lb, as compared to a capsule weight of 600 lb, the assumption of constant mass simplified the governing equations as follows:

$$I_x\dot{\omega}_x - (I_y - I_z)\omega_y\omega_z = L_x \quad (8)$$

$$I_y\dot{\omega}_y - (I_z - I_x)\omega_x\omega_z = L_y \quad (9)$$

$$I_z\dot{\omega}_z - (I_z - I_y)\omega_x\omega_y = L_z \quad (10)$$

where $L_x = F_1(t)R_1 - F_2(t)R_2$, and $F(t)$ = the thrust time function for spin motor (1 or 2). The angular velocities were determined by simultaneous integration of these equations from the following initial conditions: $(\omega_{x0}^2 + \omega_{y0}^2)^{1/2}$ = tip-off rate = $\dot{\theta}_0$, and ω_{z0} = roll rate = 0. After determining the angular velocities, the angular position of the capsule was determined as a function of time.

Thus, differences in Δt_i, t_b, and P_{av} were investigated by calculating α, for a 3σ estimate of spin motor mismatch as a function of Z, and $\dot{\theta}_0$. When the spin motors are coplanar and $\dot{\theta}_0 = 0$, there is no effect of spin-motor mismatch. This determines the optimum location of the spin motors. Figure 7 presents the results of a number of calculations for pointing error caused by spin-up. The dependence upon $\dot{\theta}_0$ becomes relatively less important as Z increases. As Z increases the differences in the spin motors are accentuated. When one motor was heated to 160°F, the change in burning rate (Fig. 3) caused increases in α even though $\int Pdt$ of the two motors was the same. This is attributable to shift in magnitude and time sequence of thrust of the motors.

Conclusions

A propellant (Aerojet AN-583-AF) has been demonstrated which provides a high-modulus, heat-sterilizable formulation useful in accurate machining of highly reproducible charges. The sterilized spin-motor firings indicate that differences in total impulse and average pressure can be maintained at or below the 1% level.

To minimize the spin-up pointing error for given spin motors, Z and $\dot{\theta}_0$ should be kept to a minimum. Significant increases in pointing error results from unequal motor temperatures even if total impulses are the same. For the geometry under consideration, increasing ϵ and η do not significantly reduce the plume impingement effects.

References

[1] Karydas, A. I. and Kato, M. T., "An Approximate Method for Calculating the Flow Field of a Rocket Exhausting into a Vacuum," Publication U-2630, June 1965, Aeronutronic Div. of Ford and Philco.

[2] Kelley, J. H. and Young, D. L., interdepartmental communication, Dec. 30, 1965, Propulsion Div., Jet Propulsion Lab.

[3] Armstrong, R. S., "Errors Associated with Spinning-Up and Thrusting Symmetric Rigid Bodies," TR 32-644, Feb. 1965, Jet Propulsion Lab., Pasadena, Calif.

[4] Dobrotin, B., privatec ommunication, June 1968, Rigid Body Spin-up Computer Program, Jet Propulsion Lab.

Streamlining Vehicles for High-Altitude Hypersonic Flight

JOHN WEBSTER ELLINWOOD*
The Aerospace Corporation, El Segundo, Calif.

Nomenclature

C = Chapman-Rubesin constant; $C = [\mu(T_r)/\mu_\infty](T_\infty/T_r)$
C_D = drag coefficient based on frontal area
$C_D{}^{fm}$ = free-molecule drag coefficient
d = $C_D{}^{fm}/C_D(\bar{v}_m,\theta)$
I = integral given by Eq. (1) and Eq. (3)
N = exponent of power-law C_D given by Eq. (2)
M_∞ = freestream Mach number
R = log $(\rho_{\max}/\rho)$
$Re_{\infty,L}$ = Reynolds number based on freestream conditions and vehicle length
T_r = reference temperature, $T_r \approx \langle T_w, T_0/4\rangle$
T_w, T_0 = surface and stagnation temperatures, respectively
$\bar{v}$ = $M_\infty(C/Re_{\infty,L})^{1/2}$
$\bar{v}_m$ = minimum $\bar{v}$
θ = cone half angle
θ_m = θ for minimum $C_D(\bar{v}_m)$
μ = air viscosity

Introduction

THE aerodynamic designer often desires to construct a vehicle with minimum drag at some flight condition. For hypersonic flight, if the altitude of interest corresponds to free-molecule flow (above about 65 naut miles for a vehicle 30 ft long) it is well known that streamlining, in the sense of increasing the length for given frontal area, does not reduce drag. The free-molecule drag coefficient $C_D{}^{fm}$, based on frontal area, is independent of shape as long as the typical body slope θ is much larger than the reciprocal speed ratio. On the other hand, for low altitudes, where the viscous boundary layer on the vehicle is thinner than the vehicle, C_D varies as θ^2, and streamlining is aerodynamically useful.

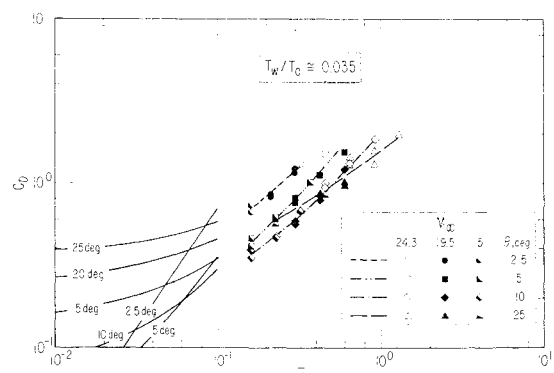

Fig. 1 Zero-lift drag coefficient of pointed cones at high altitudes.

Received June 27, 1969; revision received September 26, 1969. This work was supported by the U.S. Air Force under Contract F04701-68-C-0200.

* Member of the Technical Staff, Aerodynamics and Propulsion Research Laboratory. Member AIAA.

What is not commonly appreciated is that in between, in regions of high-altitude continuum and transitional flow, C_D for very small θ may actually exceed that for moderate θ. As altitude is increased, the drag advantage of a very slender design becomes a penalty. This Note explores the effect of streamlining, first at a given flight condition in the near-continuum regime and then over the entire upper end of the transitional flow regime.

As a model of slender vehicles, for which some theory and data are available, we limit our attention to unyawed pointed cones with semi-apex angle θ. Mirels and Ellinwood have recently theoretically determined the continuum aerodynamics for unyawed cones.[1] Their theory for C_D with a cold wall is plotted in Fig. 1 for values of the rarefaction parameter $\bar{v} \equiv M_\infty(C/Re_{\infty,L})^{1/2}$ less than 0.1. Also plotted in Fig. 1 are the most systematic of the existing experimental data for sharp cones in transitional flow.[2]

Figure 1 shows that for $0.06 < \bar{v} < 0.5$, cones with $\theta = 10°$ have the lowest C_D of those for any θ shown. In fact, $\theta = 10°$ can be shown theoretically to produce the minimum C_D when $\bar{v} = 0.1$, and by studying the experimental data, it can be inferred that the minimum C_D occurs when $\theta \approx 15°$ for $\bar{v} \approx 0.3$ and when $\theta \approx 20°$ for $\bar{v} \approx 0.6$.

These conclusions depend on the relative values of C_D for different θ, rather than on the scale of all the data or theory. The relationship between curves for different θ shown by the theory is in good agreement with that shown by the transitional data, even though the absolute level of our theory appears to be at least 30% higher than the data at $\bar{v} = 0.15$. The first experimental studies of the structure of the outer half of axisymmetric shock layers, by McCroskey, Bogdonoff, and Genchi,[3] suggest that streamwise variations in maximum density occurred for $\bar{v} \gtrsim 0.08$ for their cone ($\theta = 10°$). For these reasons the theory is not shown in Fig. 1 for $\bar{v} > 0.10$.† From Fig. 1, it is clear that theoretical models are needed that apply when $\bar{v} > 0.10$. From Ref. 3, it appears that rarefied flow models are less needed than are additional continuum flow models with improved boundary conditions.

Although Fig. 1 is directly usable for some sustained flights where $\bar{v}$ is constant, there are flight missions for which $\bar{v}$ varies and has a local minimum $\bar{v}_m$ in the range $10^{-2} < \bar{v}_m < 1$. These include skip trajectories and very low orbits of powered satellites (perigees below about 65 naut miles). For such applications, it is desirable to determine a $\bar{v}$, called $\bar{v}_{av}$, at which the optimal θ, called θ_{opt}, will be the same θ that minimizes the drag integrated over path length. One can develop a simple method for finding such a $\bar{v}_{av}$ by crudely modeling the atmospheric, trajectory, and aerodynamic characteristics as follows.

Let the density vary exponentially with radial distance r from some reference point appropriate for local atmospheric variations, such as earth oblateness and atmospheric bulge;

$$\log\,[\rho(\bar{v}_m)/\rho] = R = [r - r(\bar{v}_m)]/H$$

In addition, let the trajectory near $\bar{v}_m$ be locally parabolic (so that the path length from $\bar{v}_m$ varies as $R^{1/2}$). Then the drag integral to be minimized is

$$I(\theta) = \int_0^\infty C_D\,(\bar{v},\theta)R^{-1/2}\exp(-R)dR \qquad (1)$$

Let the speed and ambient temperature be approximately constant, so that $\bar{v}$ and R are related by $R = 2\log\,(\bar{v}/\bar{v}_m)$.

† The continuum theory also fails when velocity slip and temperature jump cannot be neglected. These effects have been shown (Appendix B of Ref. 1) to depend on a different parameter. For the cold-wall conditions of Fig. 1, the $\bar{v}$ for incipient slipping is less than 0.08 only if $\theta \lesssim 1.7°$. This angle varies as the square root of surface temperature.

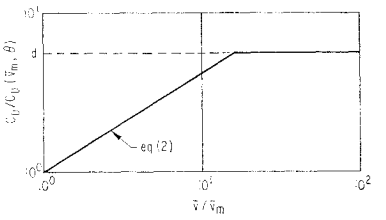

Fig. 2 Model of cone drag coefficient in transitional flow.

Finally, let $C_D(\bar{v},\theta)$ in the near-continuum and transitional regimes be approximated by a broken straight line on a log-log plot, as in Fig. 2;

$$\frac{C_D(\bar{v},\theta)}{C_D(\bar{v}_m,\theta)} = \begin{cases} (\bar{v}/\bar{v}_m)^N, & (\bar{v}/\bar{v}_m)^N < d \\ d, & (\bar{v}/\bar{v}_m)^N \geq d \end{cases} \qquad (2)$$

where $d \equiv C_D{}^{fm}/C_D(\bar{v}_m,\theta)$. This choice for $C_D(\bar{v},\theta)$ is based upon the observation from Fig. 1 that the data for C_D in transitional flow approach $C_D{}^{fm}$, as $\bar{v}$ increases, without noticeable anticipation of (nor rounding to) that value. $C_D{}^{fm}$ is expected to fall in the domain $2.0 \leq C_D{}^{fm} < 2.5$, assuming zero reciprocal speed ratio. One concludes that for sharp cones the rounding or overshoot in C_D in departing from $C_D{}^{fm}$ may not be an important feature if $C_D(\bar{v}_m,\theta) \lesssim 1$.

Combining Eqs. (1) and (2), one has

$$\frac{I(\theta)}{C_D{}^{fm}(\pi)^{1/2}} = \frac{1}{d}\left(\frac{2}{2-N}\right)^{1/2}\operatorname{erf}\left\{\left[\left(\frac{2-N}{N}\right)\log d\right]^{1/2}\right\} + \operatorname{erfc}\left[\left(\frac{2}{N}\log d\right)^{1/2}\right] \qquad (3)$$

If N is independent of θ, then one can minimize I by selecting θ equal to θ_m, the value that minimizes $C_D(\bar{v}_m,\theta)$. If instead N is a slowly decreasing function of θ, then one can minimize I by identifying $\bar{v}_{av}$, given by

$$\log(\bar{v}_{av}/\bar{v}_m) \sim \left[\frac{\partial I/\partial N}{\partial I/\partial(1/d)}\right]_m d(\theta_m) \qquad (4)$$

By construction, $\bar{v}_{av}$ is that average flight condition for which the locally optimal θ proves to be the over-all optimum θ; i.e., that which results in the lowest drag integrated over flight paths where $\bar{v}_m$ is the minimum $\bar{v}$.

Combining Eqs. (3) and (4), one has

$$\log\frac{\bar{v}_{av}}{\bar{v}_m} \sim \frac{1}{2(2-N)} - \left[\frac{\log d(\theta_m)}{N(2-N)}\right]^{1/2} \times \frac{[d(\theta_m)]^{1-2/N}}{\operatorname{erf}\{[(2-N)N^{-1}\log d(\theta_m)]^{1/2}\}} \qquad (5)$$

This result (Fig. 3) depends only on $N(\theta_m)$ and $d(\theta_m)$ and hence is in a form convenient to apply. One might think it should also depend upon other parameters (such as earth oblateness, atmospheric bulge, trajectory curvature and inclination, and density scale height). These have been accounted for but do not appear explicitly in the first-order estimate presented.

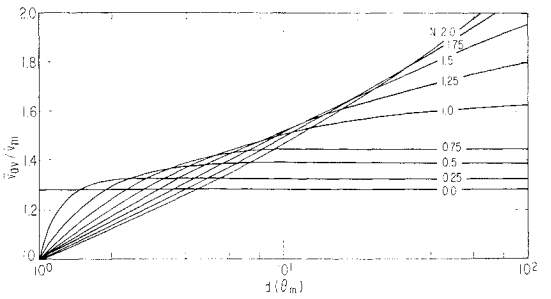

Fig. 3 Average flight condition $\bar{v}_{av}$ from Eq. (5).

In summary, the drag coefficient of slender bodies of revolution in the hypersonic near-continuum and transitional regimes has a minimum for $\theta = O(1)$. Analytic flow models that apply for $\bar{v} > 0.10$ (forward of the strong-interaction regime) are clearly needed. A first-order estimate of an average flight condition for skip trajectories and very low orbits of powered satellites is presented that depends on the drag-coefficient curve, but not on the trajectory or atmospheric details.

References

[1] Mirels, H. and Ellinwood, J. W., "Viscous Interaction Theory for Slender Axisymmetric Bodies in Hypersonic Flow," *AIAA Journal*, Vol. 6, No. 11, Nov. 1968, pp. 2061–2070.

[2] Kussoy, M. I. and Horstman, C. C., "Cone Drag in Rarefied Hypersonic Flow," AIAA Paper 69-140, New York, 1969.

[3] McCroskey, W. J., Bogdonoff, S. M., and Genchi, A. R., "Leading Edge Flow Studies of Sharp Bodies in Rarefied Hypersonic Flow," *5th International Symposium on Rarefied Gas Dynamics*, Vol. II, Academic Press, New York, 1967, pp. 1047–1066.

Nonlinear Ballistic Wind Compensation of Unguided Ballistic Rocket Systems

GERALD G. WILSON*
Sandia Laboratories, Albuquerque, N. Mex.

Nomenclature

D	=	deflection normal to corrected azimuth, or constant related to range, m
K	=	constants related to nonlinear coefficients, sec, or empirical equations, m/sec
l	=	exponent related to nominal range
m,n	=	exponents related to down- and cross-range wind effects, respectively
R	=	range, m
u,v	=	east-west (or parallel) and north-south (or normal) ballistic wind velocity components, respectively, m/sec
V	=	total ballistic wind velocity, m/sec
X,Y,Z	=	axes, positive northward, eastward, and downward, respectively, m
θ	=	launcher elevation angle measured from horizontal, deg
λ	=	directions from which the ballistic wind blows, deg
η	=	launcher azimuth angle, deg

Superscript

$'$	=	combined constants

Subscripts

0	=	nominal no-wind or condition required for vertical launcher setting
N	=	nominal or normal component
P	=	parallel component
K	=	constant associated with range
1,2	=	constant associated with down- and cross-range wind effect, respectively

Introduction

IMPACT-POINT prediction for unguided ballistic rocket systems, in the presence of surface winds, must involve solution of the six-degree-of-freedom equations of motion.[1,2]

Received August 13, 1969; revision received September 29, 1969. This work was supported by the U. S. Atomic Energy Commission.

* Staff Member in the Aerothermodynamic Projects Department. Associate AIAA.

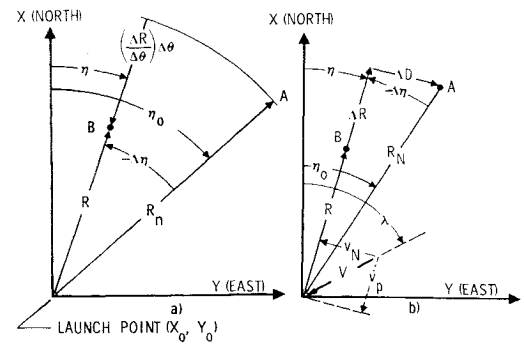

Fig. 1 Schematics of rocket trajectories without and with a ballistic wind.

The effects of system tolerances on trajectory dispersion can be reduced by aerodynamically designing the system to have a large static margin at rocket ignition. However, a large static margin at launch causes the wind effects to become a major contributor to dispersion. Vehicle dispersion can be further reduced by using both an induced roll rate and a launcher with rail guidance[3]; however, a maximum of ~5m of rail guidance is effective with most unguided systems. Numerous methods for determining launcher settings have been proposed (e.g., Refs. 4–8). These methods involve using point mass trajectories for wind effects, assuming that down-range and cross-range wind effects are identical for all elevations angles of interest, "near-vertical" launches, extensive and time-consuming graphical techniques, and other undesirable features. This Note presents a linear wind compensation method used very successfully by Sandia Laboratories since 1959.† The linear technique is extended to account for the nonlinear changes in down- and cross-range wind effects with elevation angle, and is used to derive a form of the empirical nonlinear equations established by Walker.[5]

Equations with Linear Wind Effects Coefficients

It is assumed that the altitude-wind profile obtained near the time of launch is effectively reduced by a wind-weighting system to a ballistic wind of magnitude V blowing at an angle λ. All angles are measured by the right-hand rule from the X axis, with the exception of the elevation angle θ, which is measured positive-upward from the X, Y plane. Instead of using the X, Y, Z coordinates, we use θ, range R, and deflection from the corrected azimuth D to specify the vehicle location. Figure 1a shows the projection of ballistic rocket trajectories onto the X, Y plane. When no ballistic wind is present, the R for a new launcher setting (η,θ) may be obtained by

$$R = R_N + (\Delta R/\Delta\theta)\Delta\theta = R_N + (\Delta R/\Delta\theta)(\theta - \theta_0) \quad (1)$$

where R_N and θ_0 are the nominal values, and $\Delta R/\Delta\theta$ is negative for a positive $\Delta\theta$ at large θ's. [For θ's below the θ for maximum range $(\Delta R/\Delta\theta)$ changes sign.]

When a ballistic wind acts on the system (Fig. 1b), the launcher, to compensate, must be moved through $\Delta\eta$ and $\Delta\theta$; the correct changes will cause the vehicle to pass through the nominal aiming point A. Expressions for ΔD and ΔR are obtained from Fig. 1b, and the expression for ΔR is combined with Eq. (1) to give

$$\Delta D = -R_N s\Delta\eta \quad (2)$$

$$\Delta R = R_N(c\Delta\eta - 1) - (\Delta R/\Delta\theta)\Delta\theta \quad (3)$$

† The original equations using linear (or constant) coefficients were developed by H. A. Wente, Staff Member, Aerothermodynamics Projects Department, Sandia Laboratories, Albuquerque, N. Mex.